

PREPARED FOR SUBMISSION TO JINST

INSTR17: INSTRUMENTATION FOR COLLIDING BEAM PHYSICS

27 FEBRUARY – 3 MARCH, 2017

NOVOSIBIRSK, RUSSIA

The MEGII detector

P.W. Cattaneo^a on behalf of the MEG II collaboration

^aINFN Pavia, Via Bassi 6, I-27100 Pavia, Italy

E-mail: paolo.cattaneo@pv.infn.it

ABSTRACT: We present a report of the MEG II experiment, the upgrade of MEG, whose goal is to search for the forbidden decay $\mu^+ \rightarrow e^+\gamma$ with increased precision. After having briefly reviewed the motivation for such a search and the current limit due to MEG, we present the conceptual design of the detector detailing for each subdetector the motivations and the extent of the upgrade and the expected resolution improvements. Novel subdetectors and calibration hardware are introduced. We conclude with the expected sensitivity of the MEGII experiment.

Contents

1	Introduction	1
2	Search for the $\mu^+ \rightarrow e^+\gamma$ decay	1
3	The design of the MEG II detector	2

1 Introduction

The experimental upper limits established in searching for cLFV processes with muons, including the $\mu^+ \rightarrow e^+\gamma$ decay, are shown in Fig. 1. ‘Surface’ muon beams (i.e. beams of muons originating in the decay of π^+ ’s that stopped in the surface of the pion production target) with a monochromatic momentum of ~ 29 MeV/ c , offer the highest muon stop densities obtainable at present.

The MEG experiment [1] at the Paul Scherrer Institute (PSI, Switzerland) used the world’s most intense beam with a stopping intensity of 3×10^7 μ^+ /s in the period 2009-2013. The signal of the possible two-body $\mu^+ \rightarrow e^+\gamma$ decay at rest is distinguished from the background by measuring the photon energy E_γ , the positron momentum p_{e^+} , their relative angle $\Theta_{e^+\gamma}$ and timing $t_{e^+\gamma}$ with the best possible resolutions.¹

2 Search for the $\mu^+ \rightarrow e^+\gamma$ decay

The $\mu^+ \rightarrow e^+\gamma$ is practically forbidden in the Standard Model (SM). Even in presence of massive neutrinos, the SM predicts a $\mathcal{B}(\mu \rightarrow e\gamma)$ below 10^{-50} , which cannot be experimentally observed. Processes with charge Lepton Flavour Violation are therefore clean channels to look for possible new physics beyond the SM (BSM). Many BSM models predict a measurable value of $\text{BR}(\mu \rightarrow e\gamma) \geq 10^{-14}$ [2–6]. On the basis of these theoretical predictions the MEG collaboration suggested [7] to extend the sensibility of a $\mu \rightarrow e\gamma$ search to $\sim 10^{-13}$.

In the search of this decay positive muons at rest are stopped in a target. The kinematic of the signal events is a very simple double body decay with the energies of the e^+ and of the γ equal to half of the rest muon mass m_μ . The particles are emitted in opposite directions. The background comes from radiative muon decay $\mu^+ \rightarrow e^+\nu\bar{\nu}\gamma$ (RMD) close to the kinematic limit and, more relevant, accidental coincidences from decays of different muons.

The MEG experiment took data in the years 2009-2013 [1] improving the limit on this decay by almost a factor of 30, down to $\text{BR}(\mu \rightarrow e\gamma) < 4.2 \cdot 10^{-13}$ [8–11]. This result is presented in Fig. 1 together with the results of previous cLFV searches.

After the end of the run, the collaboration launched a redesign of the experiment, now called MEG II, for further improving the limit by almost an order of magnitude. The experiment has been

¹In the following we will indicate the (1σ) resolution on a variable with a Δ in front of that variable

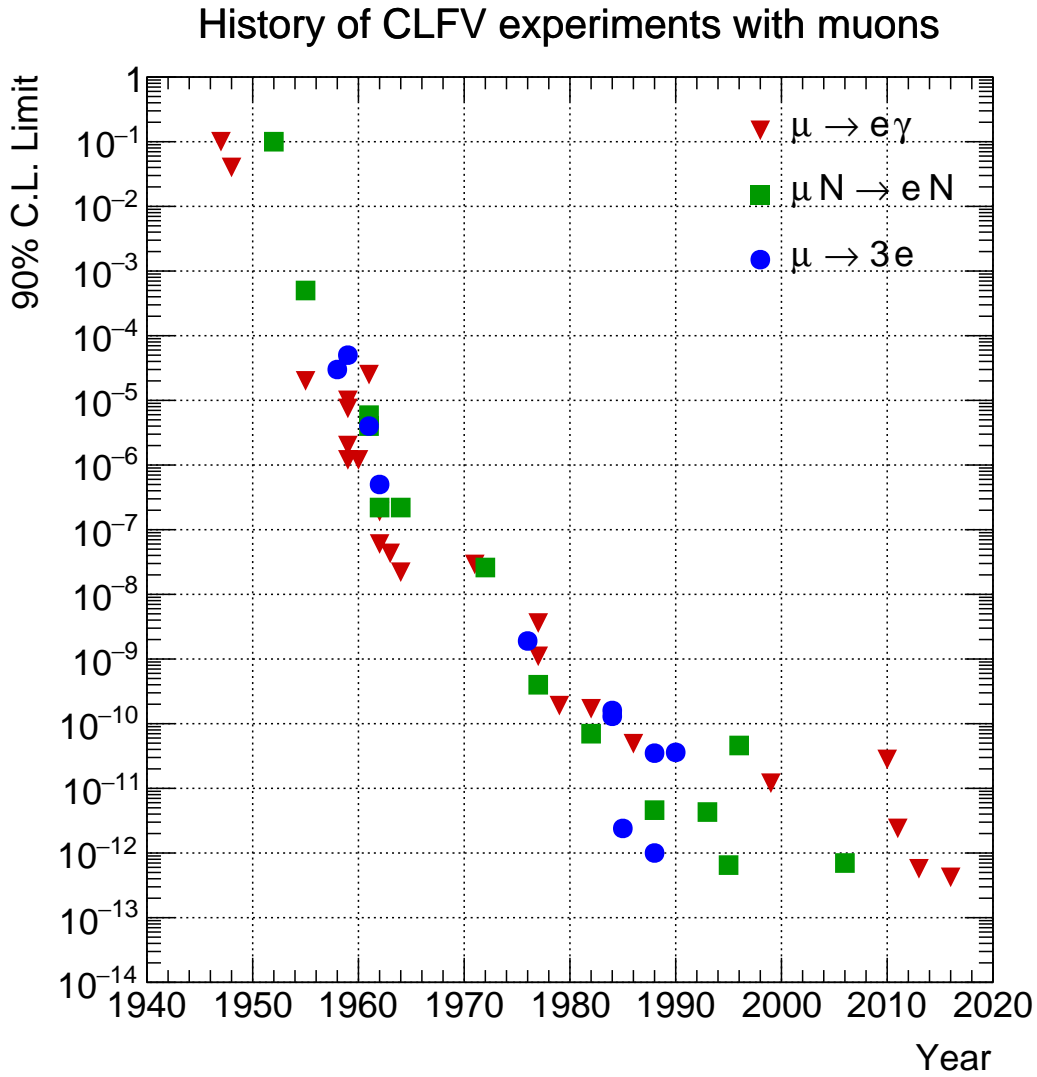


Figure 1. Upper limits on cLFV processes as a function of the year.

redesigned, some parts refurbished, some designed from scratch, based on the experience acquired during the MEG run. After several years of R&D and beam tests the collaboration is ready for data taking next year. We estimate that three full years of data taking are required to reach the design sensitivity of $\sim 5 \cdot 10^{-14}$.

3 The design of the MEG II detector

The MEG II detector design is based on the MEG detector design [1]. The MEG experiment exploits a surface μ^+ high-intensity beam produced at the $\pi E5$ channel at PSI. This beam is transported onto a thin ($210 \mu\text{m}$) stopping target located at the center of a superconducting magnet generating a gradient magnetic field. This gradient field is shaped in such a way to sweep rapidly e^+ emitted

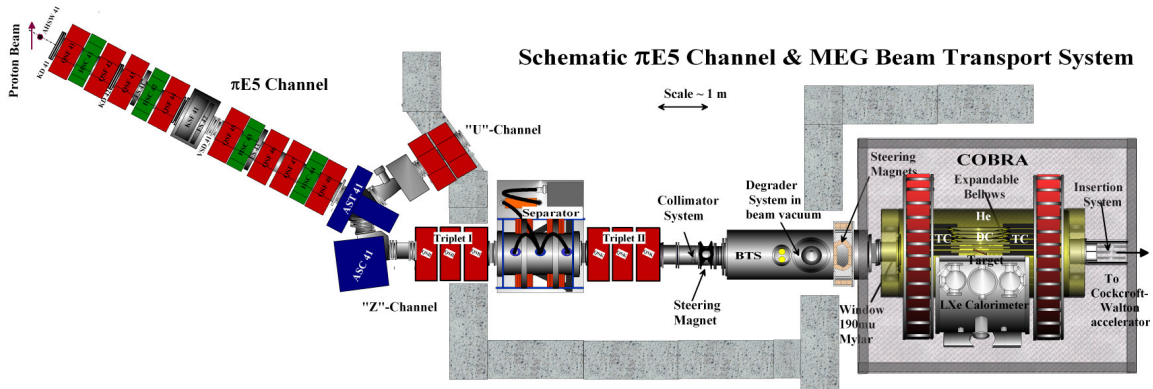


Figure 2. MEG Beam line with the $\pi E5$ channel and MEG detector system incorporated in and around the COBRA magnet.

at polar angle close to 90° and to guarantee bending radius weakly dependent on the polar angle emission.

The photon from the decay is detected by a large liquid xenon detector read out by PMTs measuring the energy, interaction time and position. The positron momentum, direction and emission vertex on the target are measured by a set of drift chambers embedded in the magnetic field. The positron decay time is measured by two barrel shaped sets of scintillator bars read out by PMTs (TC) [12].

The beam line, depicted in Fig.2 as well as the COBRA magnet are retained in MEG II, while a thinner target ($140 \mu\text{m}$) has been selected to reduce multiple scattering and therefore the positron angular resolution. The positron measuring part has been redesigned completely to overcome some of the problems that emerged during the MEG run.

The tracking detector in MEG II is a single-volume Cylindrical Drift Chamber (CDCH), whose design is optimized to satisfy the fundamental requirements of high transparency and low multiple scattering contribution for 50 MeV positrons, sustainable occupancy (at $\sim 7 \times 10^7 \mu^+/\text{s}$ stopped on target) and fast electronics for cluster timing capabilities. A sketch of the CDCH embedded in the MEG II detector is visible in Fig.3 while the results of Monte Carlo simulations of the momentum and angle resolutions are in Fig. 4.

In MEG II the TC is replaced by the pixelated Timing Counter (pTC). The pTC consists of two sets of scintillator pixels (256 each) approximately barrel shaped, each pixel read out by two sets of Silicon PhotoMultipliers (SiPM) connected in parallel positioned at opposite sides of the pixel [13–16]. A design of the pTC is in Fig. 5 and an example of a simulated signal is in Fig. 6. An advantage of this configuration is that the positron timing is measured by many (in average ~ 7) pixels and the resolution is improved by averaging down to ~ 30 ps. This resolution has been obtained in beam tests.

The LXe detector has been retained as a photon detector (see Fig .7). It has been upgraded substituting the PMTs reading the front face with SiPMs. This brings important improvements in photon position and timing resolution and in resolving closely spaced photons as shown in Fig. 8.

A new subdetector added to MEG II is the downstream RDC detector. It is capable of identifying

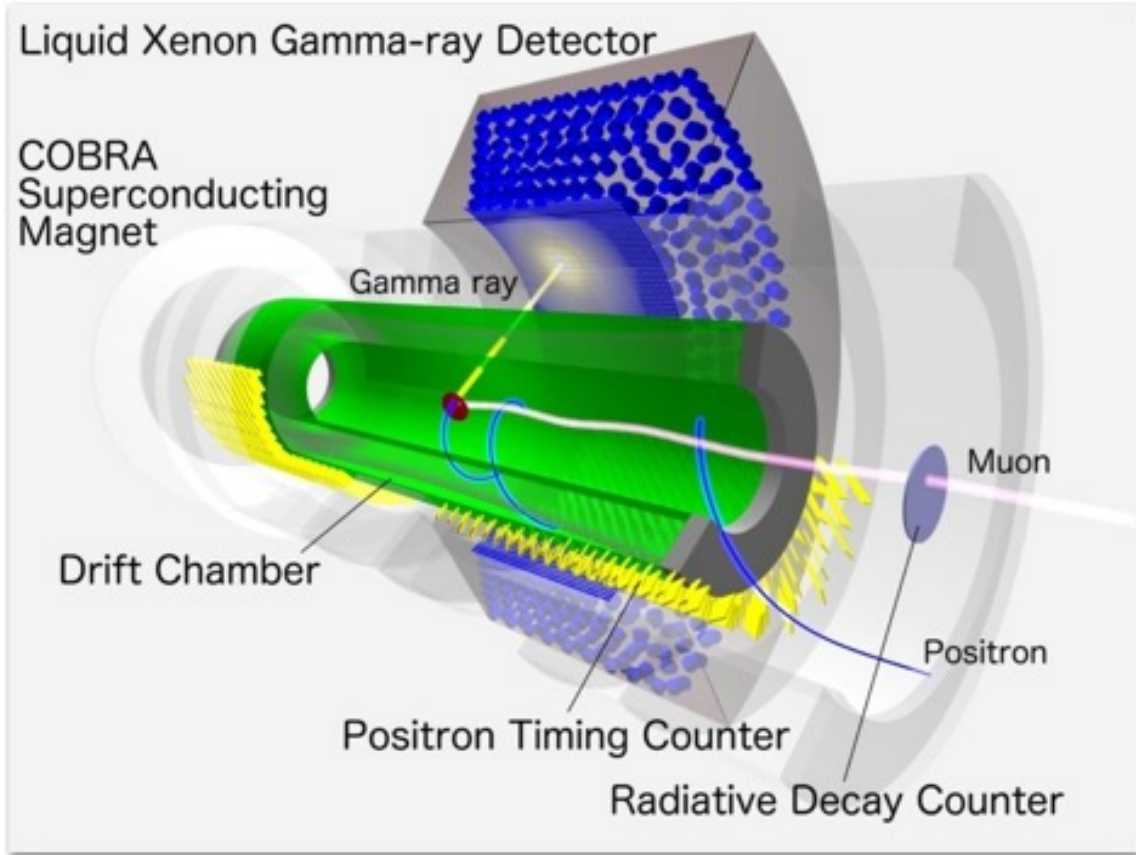


Figure 3. A sketch of the MEG II experiment. The CDCH in green

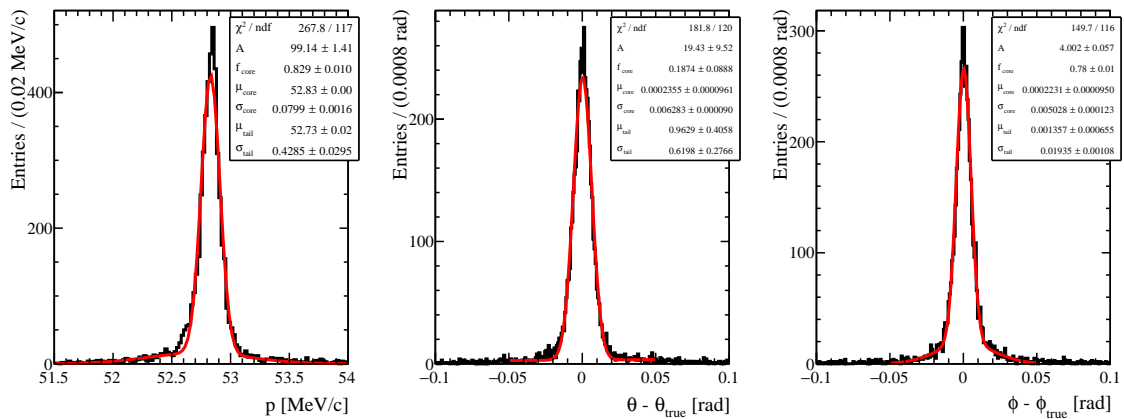


Figure 4. Expected MEG II CDCH momentum and angle resolutions, from a simulation having as inputs the results of the tests with prototypes.

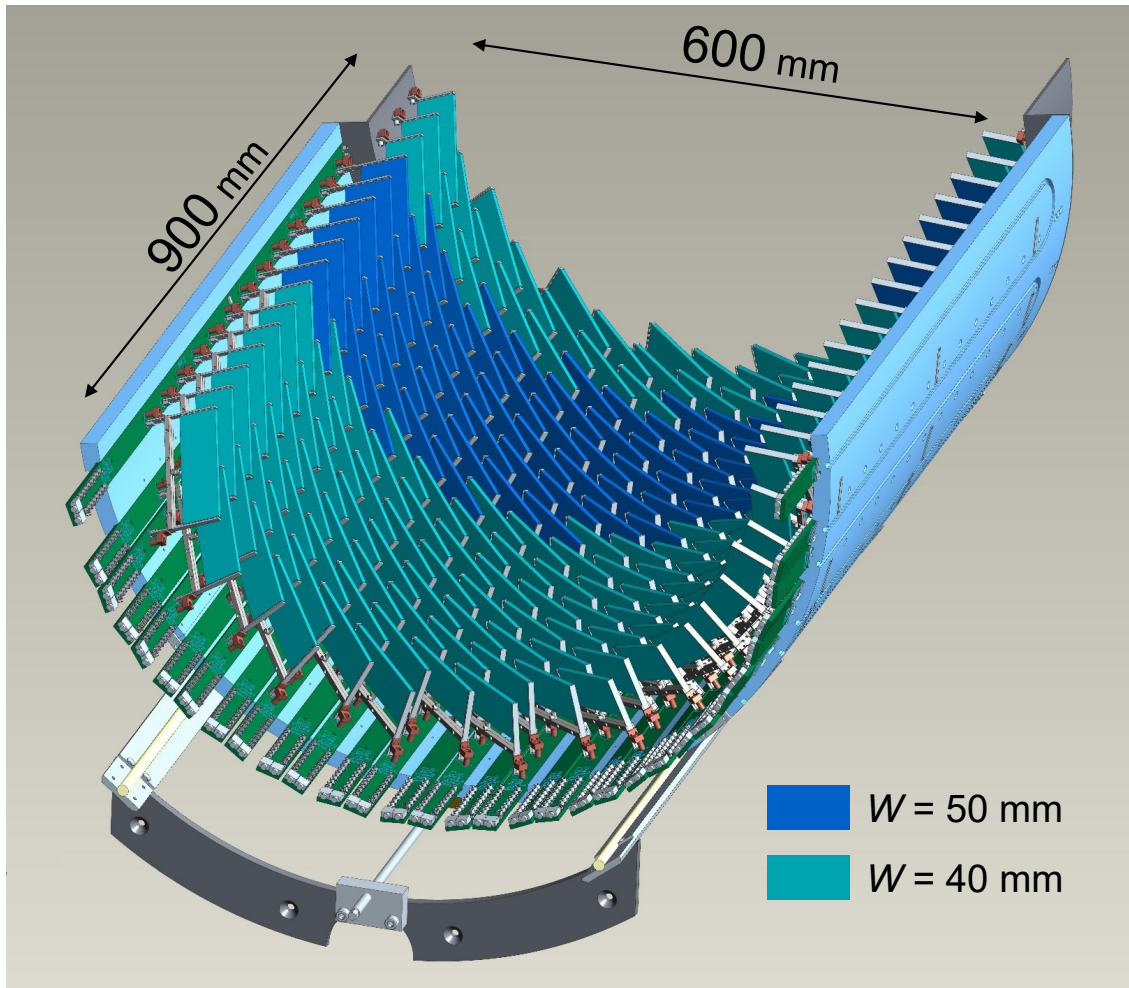


Figure 5. Design of downstream pTC super-module.

a fraction of the RMD decays with the photon energy close to the kinematic limit, which are the dominant source of background photons for accidental coincidences. The basic concept is depicted in Fig. 9. The detector consists of a plane of plastic scintillator plates for position measurement followed by a calorimeter based on LYSO crystals for energy measurements, both detectors are read out by SiPMs.

A crucial part of the experiment is the calibration and monitoring systems, some of them requiring dedicated hardware, to control over the lifetime of the experiment the responses of the subdetectors. In Table 1 the list of calibration of tools to be used in MEG II is presented. As an example, in Fig.10 the result of a novel device for monitoring the beam spot based on scintillating fibers is presented.

In Table 2 the resolutions and efficiencies required by the calculation of the sensitivity are presented for MEG (measured) and MEG'II (expected); the improvements are clear. In Fig 11 the MEG II sensitivity versus data taking time is shown. The MEG final limit ($4.3 \cdot 10^{-14}$) and the MEG II expectation for three years of data taking are shown.

Table 1. The calibration tools of the MEG II experiment.

Process	Energy	Main Purpose	Frequency
Cosmic rays	atmospheric μ^\pm	Wide spectrum $O(\text{GeV})$	LXe-CDCH relative position CDCH alignment Annually
Charge exchange	$\pi^- p \rightarrow \pi^0 n$ $\pi^0 \rightarrow \gamma\gamma$	55, 83, 129 MeV γ	LXe purity LXe energy scale/resolution On demand Annually
Radiative μ -decay	$\mu^+ \rightarrow e^+ \nu \bar{\nu} \gamma$	Photons > 40 MeV, Positrons > 45 MeV	LXe-pTC relative timing Normalisation Continuously
Normal μ -decay	$\mu^+ \rightarrow e^+ \nu \bar{\nu}$	52.83 MeV end-point e^+ 's	CDCH energy scale/resolution CDCH energy scale/resolution CDCH and target alignment pTC time/energy calibration Normalisation Continuously Continuously
Mott positrons	e^+ target $\rightarrow e^+$ target	≈ 50 MeV e^+ 's	CDCH energy scale/resolution CDCH alignment Annually
Proton accelerator	${}^7\text{Li}(p, \gamma){}^8\text{Be}$ ${}^{11}\text{B}(p, \gamma){}^{12}\text{C}$	14.8, 17.6 MeV photons 4.4, 11.6, 16.1 MeV photons	LXe uniformity/purity LXe-pTC timing Weekly Weekly
Neutron generator	${}^{58}\text{Ni}(n, \gamma){}^{59}\text{Ni}$	9 MeV photons	LXe energy scale Weekly
Radioactive source	${}^{241}\text{Am}(\alpha, \gamma){}^{237}\text{Np}$	5.5 MeV α 's	LXe PMT/SiPM calibration LXe purity Weekly
Radioactive source	${}^9\text{Be}(\alpha{}^{241}\text{Am}, n){}^{12}\text{C}^*$ ${}^{12}\text{C}^*(\gamma){}^{12}\text{C}$	4.4 MeV photons	LXe energy scale On demand
Radioactive source	${}^{57}\text{Co}(\text{EC}, \gamma){}^{57}\text{Fe}$	136 (11 %), 122 keV (86 %) X-rays	LXe-spectrometer alignment Annually
LED		UV region	LXe PMT/SiPM calibration Continuously
Laser		401 nm	pTC inter-counter timing Continuously

Table 2. Resolutions (Gaussian σ) and efficiencies of MEG II compared with those of MEG

PDF parameters	MEG	MEG II
E_{e^+} (keV)	380	130
θ_{e^+} (mrad)	9.4	5.3
ϕ_{e^+} (mrad)	8.7	3.7
z_{e^+}/y_{e^+} (mm) core	2.4/1.2	1.6/0.7
E_γ (%) ($w > 2$ cm)/($w < 2$ cm))	2.4/1.7	1.1/1.0
$u_\gamma, v_\gamma, w_\gamma$ (mm)	5/5/6	2.6/2.2/5
$t_{e^+\gamma}$ (ps)	122	84
Efficiency (%)		
Trigger	≈ 99	≈ 99
Photon	63	69
e^+	30	70

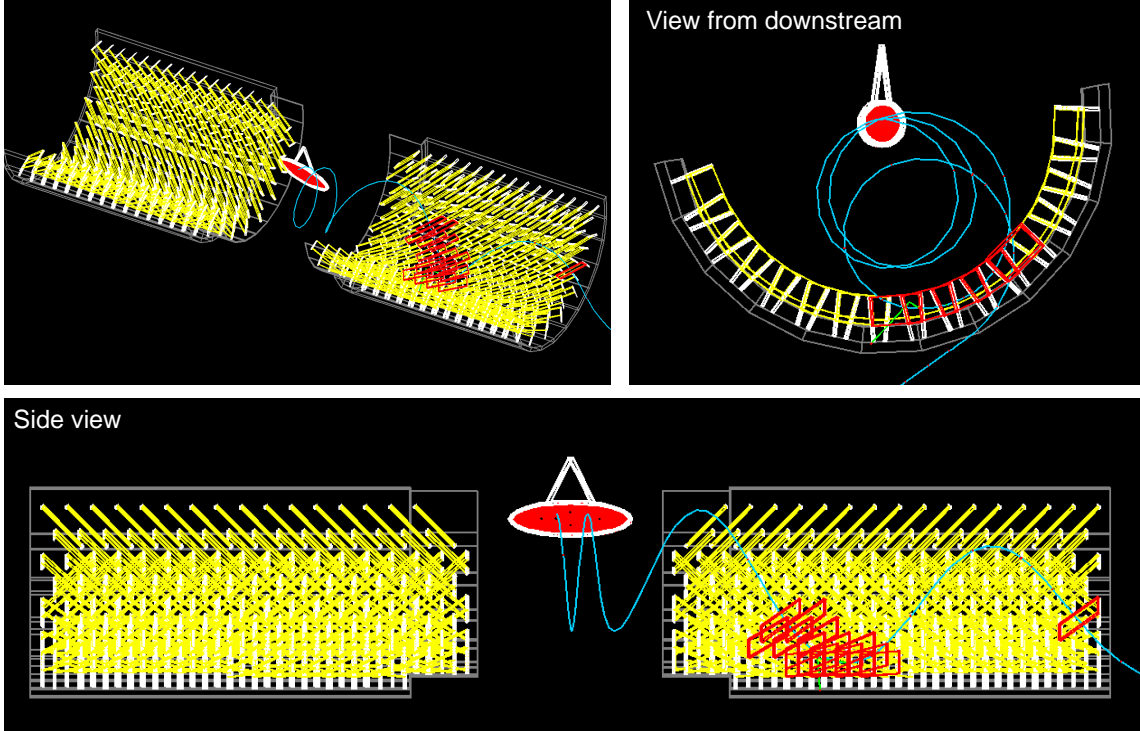


Figure 6. An example of hit pattern by a simulated signal e^+ . CDCH is not drawn in these figures.

Acknowledgments

We are grateful for the support and co-operation provided by PSI as the host laboratory and to the technical and engineering staff of our institutes.

References

- [1] J. Adam et al., *The MEG detector for $\mu^+ \rightarrow e^+ \gamma$ decay search*, *Eur. Phys. J. C* **73** (2013) 2365, [[1303.2348](#)].
- [2] R. Barbieri and L. Hall, *Signals for supersymmetric unification*, *Phys. Lett. B* **338** (1994) 212, [[hep-ph/9408406](#)].
- [3] J. Hisano, K. Kurosawa and Y. Nomura, *Large squark and slepton masses for the first-two generations in the anomalous $U(1)$ SUSY breaking models*, *Phys. Lett. B* **445** (1999) 316–322, [[hep-ph/9810411](#)].
- [4] L. Calibbi, A. Faccia, A. Masiero and S. K. Vempati, *Lepton flavor violation from supersymmetric grand unified theories: where do we stand for MEG, PRISM/PRIME, and a super flavor factory*, *Phys. Rev. D* **74** (2006) 116002, [[hep-ph/0605139](#)].
- [5] L. Calibbi, M. Frigerio, S. Lavignac and A. Romanino, *Flavour violation in supersymmetric $SO(10)$ unification with a type II seesaw mechanism*, *J. High Energy Phys.* **0912** (2009) 057, [[0910.0377](#)].
- [6] L. Calibbi, D. Chowdhury, A. Masiero, K. Patel and S. Vempati, *Status of supersymmetric type-I seesaw in $SO(10)$ inspired models*, *J. High Energy Phys.* **1211** (2012) 040, [[1207.7227](#)].

- [7] A. M. Baldini, A. De Bari, L. Barkov, C. Bemporad, P. Cattaneo, G. Cecchet et al., “The MEG experiment: search for the $\mu^+ \rightarrow e^+ \gamma$ decay at PSI.” Research Proposal to INFN, https://meg.web.psi.ch/docs/prop_infn/nproposal.pdf, Dec., 2002.
- [8] MEG COLLABORATION collaboration, J. Adam et al., *A limit for the $\mu \rightarrow e \gamma$ decay from the MEG experiment*, *Nucl. Phys. B* **834** (2010) 1–12, [[0908.2594](#)].
- [9] MEG COLLABORATION collaboration, J. Adam et al., *New limit on the lepton-flavor-violating decay $\mu^+ \rightarrow e^+ \gamma$* , *Phys. Rev. Lett.* **107** (2011) 171801, [[1107.5547](#)].
- [10] MEG COLLABORATION collaboration, J. Adam et al., *New constraint on the existence of the $\mu^+ \rightarrow e^+ \gamma$ decay*, *Phys. Rev. Lett.* **110** (2013) 201801, [[1303.0754](#)].
- [11] MEG collaboration, A. M. Baldini et al., *Search for the lepton flavour violating decay $\mu^+ \rightarrow e^+ \gamma$ with the full dataset of the MEG experiment*, *Eur. Phys. J. C* **76** (2016) 434, [[1605.05081](#)].
- [12] M. De Gerone, S. Dussoni, K. Fratini, F. Gatti, R. Valle et al., *Development and commissioning of the Timing Counter for the MEG Experiment*, *IEEE Trans. Nucl. Sci.* **59** (2012) 379–388, [[1112.0110](#)].
- [13] W. Ootani, *Development of pixelated scintillation detector for highly precise time measurement in MEG upgrade*, *Nucl. Instrum. Methods A* **732** (Dec., 2013) 146–150.
- [14] M. De Gerone et al., *Design and test of an extremely high resolution Timing Counter for the MEG II experiment: preliminary results*, *J. Instrum.* **9** (2014) C02035, [[1312.0871](#)].
- [15] P. W. Cattaneo, M. De Gerone, F. Gatti, M. Nishimura, W. Ootani et al., *Development of high precision timing counter based on plastic scintillator with SiPM readout*, *IEEE Trans. Nucl. Sci.* **61** (2014) 2657–2666, [[1402.1404](#)].
- [16] M. Nishimura et al., *Pixelated positron timing counter with SiPM-readout scintillator for MEG II*

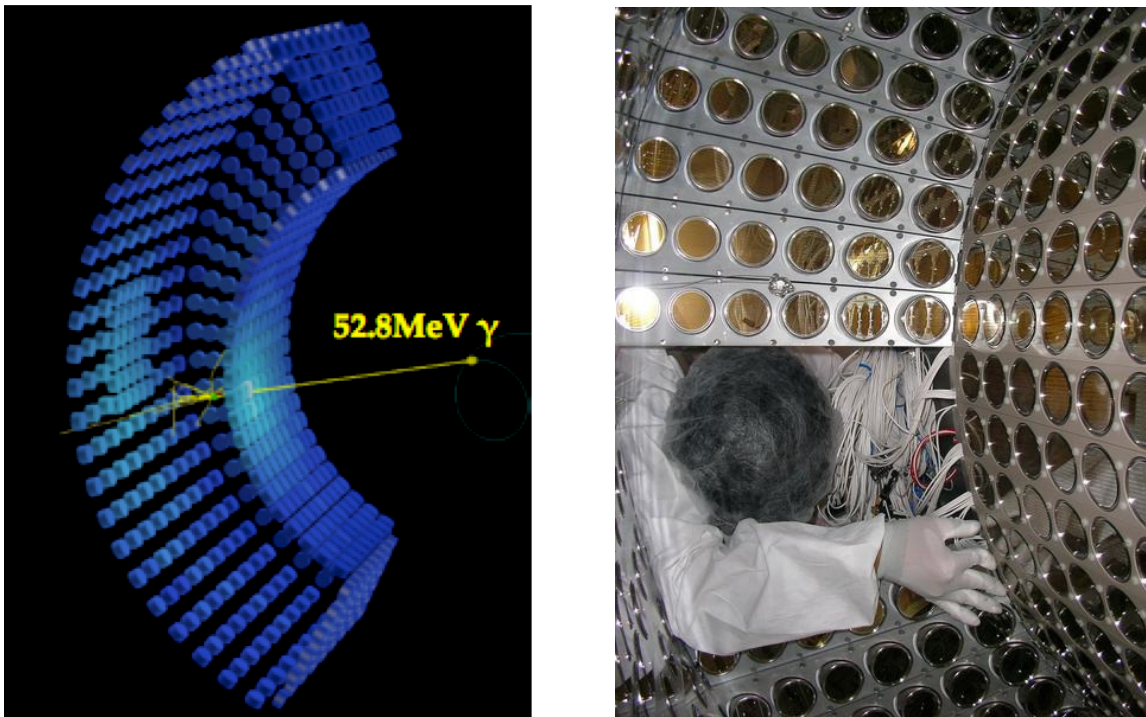


Figure 7. MEG LXe photon detector with 900 ℓ LXe surrounded by 846 UV-sensitive PMTs.

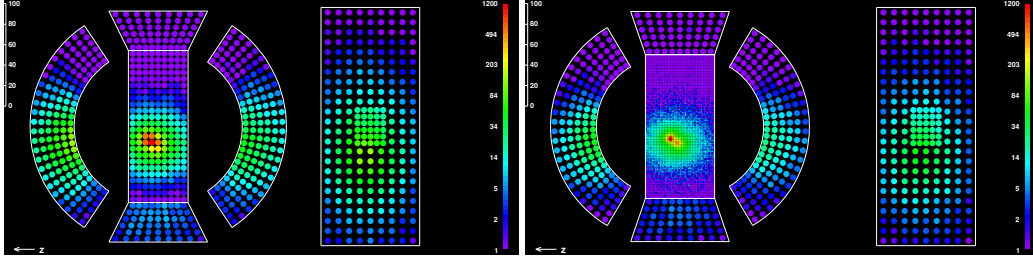


Figure 8. Example of scintillator light distributions seen by photo-sensors in case of (left) PMTs and (right) smaller photo-sensors ($12 \times 12 \text{ mm}^2$) on the photon entrance face against the same MC event.

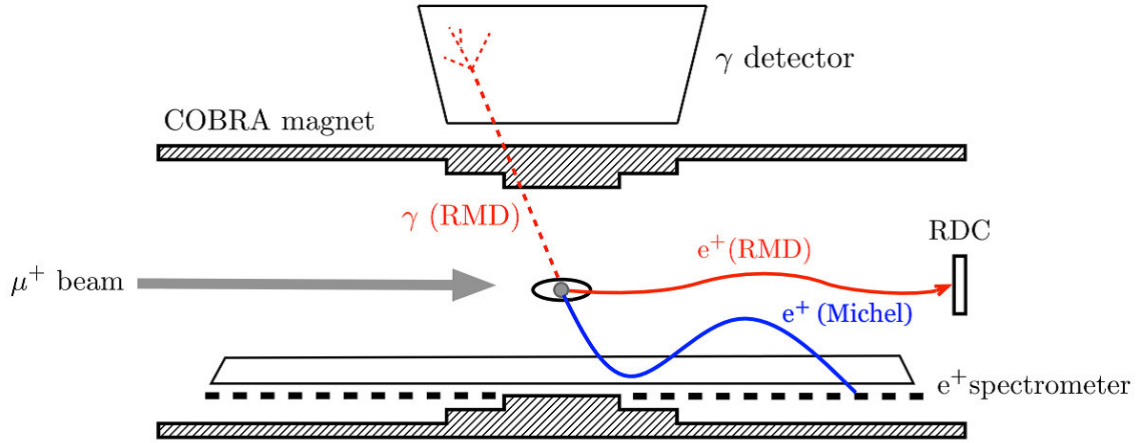


Figure 9. Schematic view of the detection of RMD with the RDC detector.

experiment, in *Proceedings 4th Int. Conf. on New Photo-Detectors*, (Moscow, Russia.), p. PoS(PhotoDet 2015)011, July, 2016.

- [17] MEG COLLABORATION collaboration, A. M. Baldini et al., *Search for the lepton flavour violating decay $\mu^+ \rightarrow e^+ \gamma$ with the full dataset of the MEG experiment*, *Eur. Phys. J. C* **76** (2016) 434, [[1605.05081](#)].

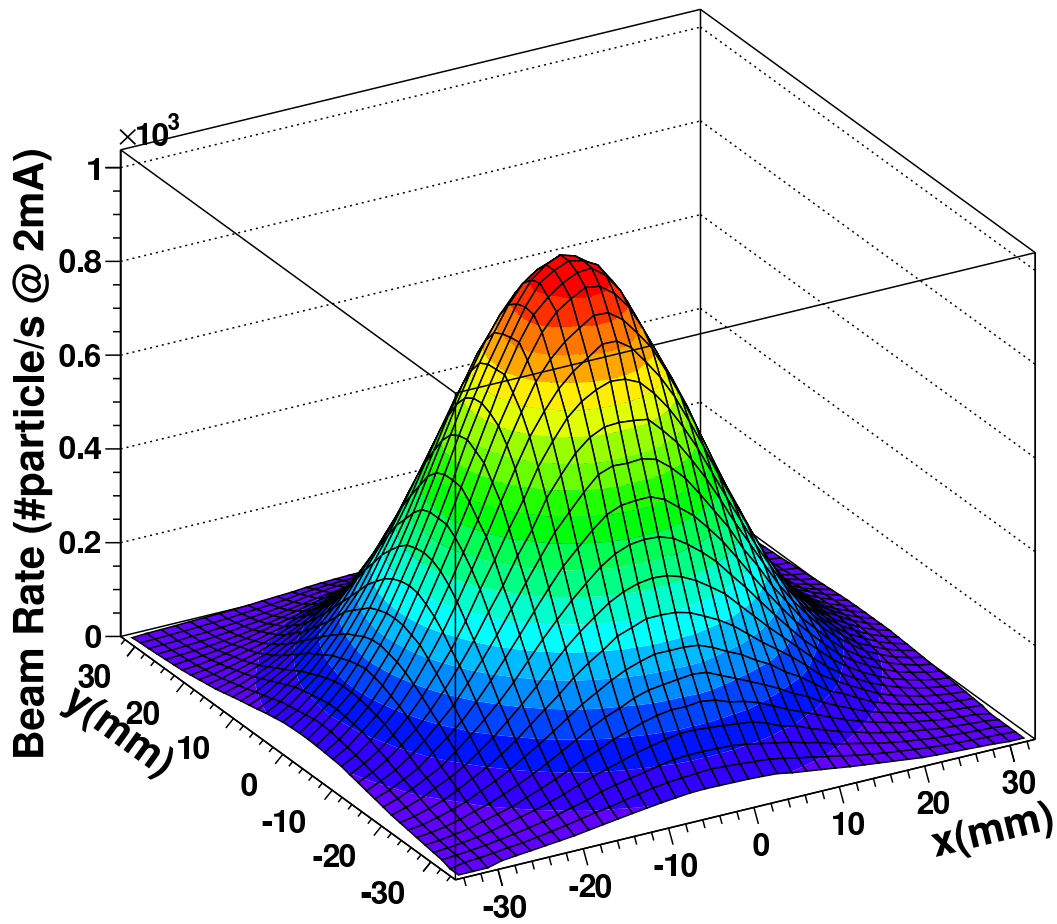


Figure 10. Positive muon beam profile and rate as measured along the π E5 beam line.

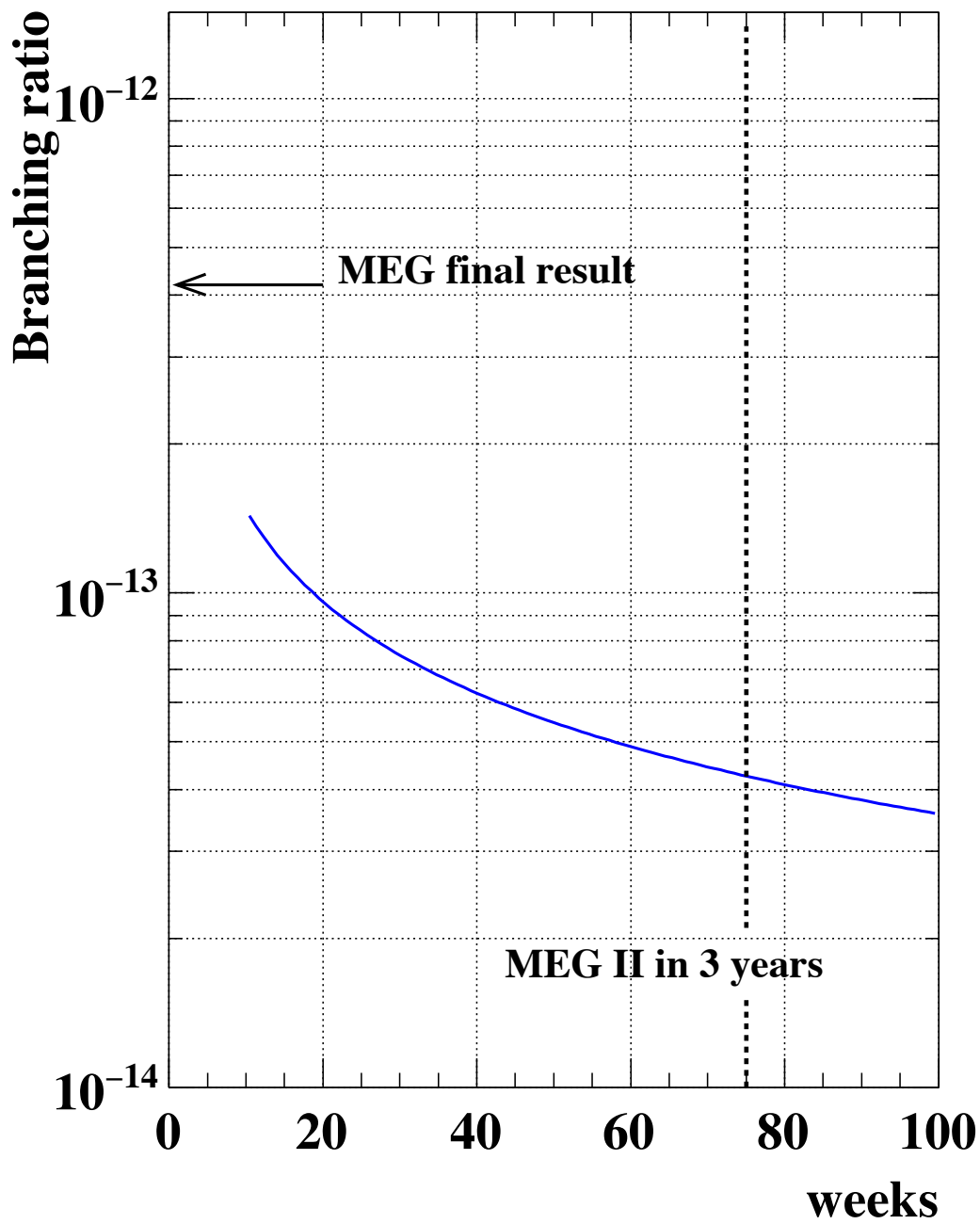


Figure 11. Expected sensitivity of MEG II as a function of the DAQ time compared with the bounds set by MEG [17]. Assuming 25 DAQ weeks per year, we expect a 90%-CL UL $\mathcal{B}(\mu^+ \rightarrow e^+\gamma) < 4.3 \times 10^{-14}$ in three years.